Continuous chromatographic separation through simulated moving beds under linear and nonlinear conditions

Cristiano Migliorini[a], Marco Mazzotti[a], Massimo Morbidelli[b],*

[a]*ETH Zürich, Institut für Verfahrenstechnik, Sonneggstrasse 3, CH-8092 Zurich, Switzerland*
[b]*ETH Zürich, Laboratorium für Technische Chemie, Universitätstrasse 6, CH-8092 Zurich Switzerland*

Abstract

Simulated Moving Bed (SMB) technology is receiving more and more attention as a convenient technique for the production scale continuous chromatographic separation of fine chemicals. Thanks to the efficient simulated countercurrent contact between the stationary and the fluid phase, SMB units can operate under high productivity overload conditions. These lead to nonlinear competitive adsorption behavior, which has to be accounted for when designing and optimising new SMB separations. The so called 'Triangle Theory', which is briefly revised here, provides explicit criteria for the choice of the operating conditions of SMB units to achieve the prescribed separation of a mixture characterized by Langmuir, modified Langmuir and bi-Langmuir isotherms. In all these cases, the effect of increasing nonlinearity of the separation, due to increased feed concentration can be predicted. In this paper, the use of this approach for the design of linear and nonlinear SMBs is considered, with reference to examples reported previously. Alternative strategies have been proposed in the literature, which are based on the use of safety factors for linear systems and on an adaptation of this for nonlinear ones. In the cases considered, which involve experimental data for a linear system and numerical experiments for a nonlinear Langmuir system, it is shown that 'Triangle Theory' allows attainment of a better understanding of and a deeper insight into the behavior of SMB units. © 1998 Elsevier Science B.V. All rights reserved.

Keywords: Preparative chromatography; Simulated moving bed chromatography; Triangle theory

1. Introduction

Continuous chromatographic separations of fine chemicals and enantiomers can be realized through the Simulated Moving Bed (SMB) technology [1–3]. Several new applications have been developed recently (cf. [4] for an updated review). These include the liquid phase separation of Tröger's base enantiomers on microcrystalline triacetylcellulose [4] and the gas phase separation of the enantiomers of the inhalation anaesthetic enflurane on a cyclodextrin based stationary phase [5]; the latter represents the first GC–SMB enantioseparation reported in the literature.

The SMB technique involves the simulated countercurrent contact between the mobile fluid phase and the stationary phase, which is most efficient in terms of separation performance, eluent consumption and productivity per unit mass of stationary phase. This can be accomplished in units constituted of a set of fixed bed chromatographic columns like that illustrated in Fig. 1, through the periodic movement of inlet and outlet ports in the same direction of the fluid flow. With reference to a binary mixture to be separated, which constitutes the Feed stream to the unit, the more adsorbable component, called A, is collected in the Extract stream, whereas the less
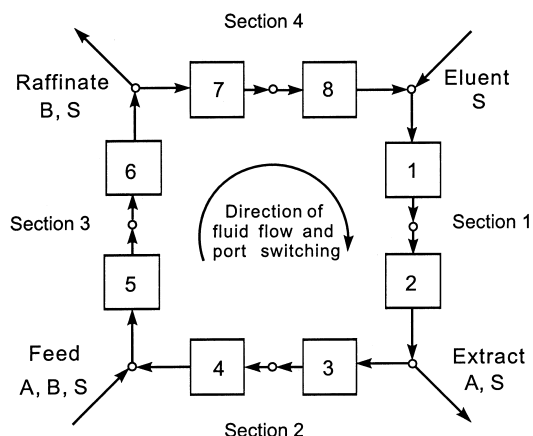
*Corresponding author.

Fig. 1. Scheme of a four-section Simulated Moving Bed unit for continuous adsorptive separations with port distribution 2-2-2-2: the binary separation of a more retained component A and a less retained component B is considered.

adsorbable one, called B, is collected in the Raffinate stream. Each section of the unit plays a specific role in the operation. The separation is performed in the two central sections. where component B is carried by the mobile phase while on the other hand component A is retained by the stationary phase. The eluant, indicated as S, is used to desorb component A from the first section, so as to regenerate the adsorbent. Finally, component B is adsorbed in the fourth section of the unit, so as to regenerate the desorbent itself.

The SMB technology constitutes a rather complex unit operation, which requires a deep understanding in order to make its use effective. To achieve this objective a rather natural approach would involve the use of a general model aimed at performing a parametric analysis of the SMB behavior. Actually, this approach was followed in earlier studies [6–8] and it is still applied to analyse different aspects of SMB performances [9–11]. However, comprehensive simulation-based analyses such as the one carried out by Zhong and Guiochon [10] highlight a rather broad range of effects due to the many parameters involved but do not provide a deep understanding of SMB behavior. To this aim a more synthetic view of the process is required. This is actually offered by the model based on Equilibrium Theory where mass transfer resistance and axial dispersion are neglected. Applying this model to

SMB units under the assumption of a Langmuir-type adsorption isotherm yields the so called 'Triangle Theory', which allows determination of optimal and robust operating conditions of SMBs to achieve the required separation specifications [12–19]. Its most important aspects are discussed in the following section. It is worth stressing that this approach allows the overload operating conditions typical of SMBs to be taken into account, which lead to nonlinear competitive adsorption behavior. This makes the approach rather powerful, particularly when compared with other approaches based on empirical adaptations of the linear criteria to the design of nonlinear SMB operations [10]. Some examples are discussed to illustrate the drastic limitations of these techniques, which can be overcome only through the proper account of the adsorption isotherm non-linearities.

2. Background on the 'Triangle Theory'

In this section we briefly review the criteria for the design of operating conditions of SMB units that have been developed under ideal conditions, i.e., neglecting axial dispersion and mass transfer resistance, hence assuming columns of infinite efficiency.

Let us consider a four-section SMB unit and the case where complete separation of a binary mixture, constituted of the more retained component A and the less retained component B, is required, i.e., the situation illustrated in Fig. 1. In the frame of Equilibrium Theory, the key operating parameters through which the separation performance can be controlled are the flow rate ratios, m_j, $j = 1, \ldots, 4$, in the four sections of the SMB units:

$$m_j = \frac{Q_j t^* - V\varepsilon^*}{V(1 - \varepsilon^*)}. \tag{1}$$

where V is the volume of the column: t^* is the switch time, i.e., the time period between two successive switches of the inlet and outlet ports; $\varepsilon^* = \varepsilon + (1 - \varepsilon)\varepsilon_p$, is the overall void fraction of the bed, with ε and ε_p being the bed void fraction and the macroporosity of the stationary phase particles, respectively; Q_j is the volumetric flow rate in the

j-th section of the SMB unit. Constraints on the values of the flow rate ratios can be determined which depend only on the parameters characterizing the adsorption equilibrium of the species to be separated. These have been derived in the most general case for a bi-Langmuir multicomponent adsorption isotherm [19] and previously for the Langmuir and the modified Langmuir isotherm [12,17]. These last two relationships represent a special case of the bi-Langmuir isotherm, with the advantage that all the results can be cast in explicit form and therefore are very simple to implement.

2.1. Langmuir isotherm

For the sake of simplicity in this work we deal with the binary Langmuir isotherm:

$$n_i = \frac{H_i c_i}{1 + K_A c_A + K_B c_B}, \quad (i = A,B), \tag{2}$$

where n_i and c_i are the adsorbed and fluid phase concentration, respectively; H_i is the Henry constant of the i-th component, i.e., the slope of the single component adsorption isotherm at infinite dilution; K_i is the equilibrium constant of the i-th component, which accounts for the competitive and overload effects. Coupling the process requirement of complete separation with the material balances at the nodes of the SMB unit and using the results of Equilibrium Theory for Langmuir systems, yields the following set of conditions that the flow rate ratios have to fulfill in order to achieve complete separation:

$$H_A < m_1 < \infty, \tag{3}$$

$$m_{2,cr}(m_2,m_3) < m_2 < m_3 < m_{3,cr}(m_2,m_3), \tag{4}$$

$$\frac{-\varepsilon_p}{1 - \varepsilon_p} < m_4 < m_{4,cr}(m_2,m_3)$$

$$= \frac{1}{2} \left\{ H_B + m_3 + K_B c_B^F (m_3 - m_2) \right.$$

$$\left. - \sqrt{[H_B + m_3 + K_B c_B^F (m_3 - m_2)]^2 - 4H_B m_3} \right\}, \tag{5}$$

where the superscript F indicates feed conditions. The constraints on m_1 and m_4 are explicit. However, the lower bound on m_1 does not depend on the other

flow rate ratios, whereas the upper bound on m_4 is an explicit function of the flow rate ratios m_2 and m_3 and of the feed composition [17]. The constraints (4) on m_2 and m_3 are implicit, but they do not depend on m_1 and m_4. Therefore, they define a unique complete separation region in the (m_2, m_3) plane, which is the triangle-shaped region *abw* drawn in Fig. 2. The boundaries of this region can be calculated explicitly in terms of the adsorption equilibrium parameters and the feed composition as follows [17]:

● Straight line wf:
$$(H_A - \omega_G(1 + K_A c_A^F))m_2 + K_A c_A^F \omega_G m_3 =$$
$$\omega_G(H_A - \omega_G) \tag{6}$$

● Straight line wb:
$$(H_A - H_B(1 + K_A c_A^F))m_2 + K_A c_A^F H_B m_3 =$$
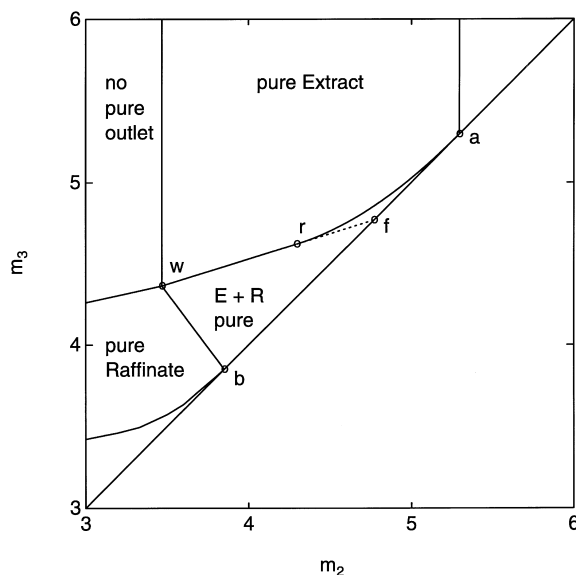$$H_B(H_A - H_B) \tag{7}$$

● Curve ra:

Fig. 2. Separation of a two component mixture using a nonadsorbable desorbent. Regions of the (m_2, m_3) plane with different separation regimes in terms of purity of the outlet streams, for a system described by the Langmuir adsorption isotherm (2): $H_A = 5.30$, $H_B = 3.85$, $K_A = 0.0321$ ml/mg, $K_B = 0.0175$ ml/mg, $c_A^F = c_B^F = 5$ mg/ml.

$$m_3 = m_2 + \frac{(\sqrt{H_A} - \sqrt{m_2})^2}{K_A c_A^F} \tag{8}$$

● Straight line ab:

$$m_3 = m_2 \tag{9}$$

The coordinates of the intersection points are given by:

point a (H_A, H_A) (10)

point b (H_B, H_B) (11)

point f (ω_G, ω_G) (12)

point r $\left(\dfrac{\omega_G^2}{H_A}, - \right.$

$$\left. \frac{\omega_G[\omega_F(H_A - \omega_G)(H_A - H_B) + H_B\omega_G(H_A - \omega_F)]}{H_A H_B(H_A - \omega_F)} \right) \tag{13}$$

point w $\left(\dfrac{H_B\omega_G}{H_A}, \dfrac{\omega_G[\omega_F(H_A - H_B) + H_B(H_B - \omega_F)]}{H_B(H_A - \omega_F)} \right)$ (14)

In the above equations ω_F and ω_G depend on the feed composition; they are the roots of the following quadratic equation, with $\omega_G > \omega_F > 0$:

$$(1 + K_A c_A^F + K_B c_B^F)\omega^2 - [H_A(1 + K_B c_B^F)$$
$$+ H_B(1 + K_A c_A^F)]\omega + H_A H_B = 0. \tag{15}$$

As illustrated in Fig. 2, the complete separation region is surrounded by three regions corresponding to three different operating regimes, i.e., the pure raffinate region, where the raffinate stream is pure but the extract is polluted by component B, the pure extract region, where only the extract is pure but not the raffinate, and the no pure outlet region, where components A and B distribute in both outlet streams. The information provided by the geometrical representation of the separation regions in the (m_2, m_3) plane in Fig. 2 are correct only if the relevant constraints on m_1 and m_4, i.e., inequalities (3) and (5), are fulfilled.

It can be seen that the vertex *w* of the complete separation region in the plane (m_2, m_3) represents

optimal operating conditions in terms of solvent consumption and productivity per unit mass of stationary phase [17]. However, by inspection of Fig. 2 it can also be observed that the slightest disturbance in process conditions, as well as the smallest error in the evaluation of the adsorption equilibrium parameters, may make the operating point leave the optimal location and move outside the complete separation region. This means that the optimal operating conditions are not robust [17]. As a consequence, in practical situations the operating point is chosen within the complete separation triangle and not on its vertex, thus reaching a compromise between separation performance, i.e., productivity and solvent requirement, and process robustness.

2.2. Competitive nonlinear adsorption equilibria

The multicomponent Langmuir adsorption isotherm (2) is the simplest nonlinear model adopted to describe adsorption equilibria. At high concentration this model accounts for saturation of the stationary phase and overload of the chromatographic column. At high dilution its behavior approaches the non-competitive linear adsorption isotherm:

$$n_i = H_i c_i \ (i = A, B) \tag{16}$$

With reference to the SMB behavior, these features imply that increasing feed concentration yields an increasing degree of nonlinearity due to the overload operating conditions of the adsorption columns. This effect is automatically accounted for by the approach summarised in the previous section, in particular by Eqs. (3)–(14), which allow the calculation of the constraints on m_1 and m_4 and the boundaries of the complete separation region in the (m_2, m_3) plane as a function of feed composition.

In order to illustrate this nonlinearity effect, let us focus on the separation of a racemic mixture, for which $c_A^F = c_B^F = c_T^F/2$ and the feed composition is characterized by the single parameter c_T^F, representing the overall feed concentration. First let us consider section 1, whose constraint (3) does not depend on feed composition. On the contrary, the upper bound on the flow rate ratio m_4 given by Eq.
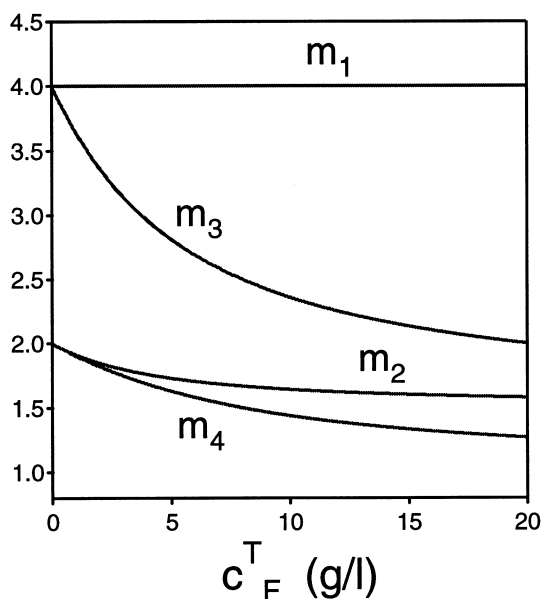
Fig. 3. Optimal values of the flow rate ratios as a function of the overall feed concentration, c_T^F; the values of m_2 and m_3 correspond to the coordinates of the optimal point W given by Eq. (14). Isotherm parameters: $H_A = 4$, $H_B = 2$, $K_A = K_B = 0.1$ ml/mg.

Fig. 4. Effect of the overall concentration of the feed mixture, c_{TF}, on the region of complete separation in the (m_2, m_3) plane. Isotherm parameters as in Fig. 3. Region L) $c_T^F \to 0$ g/l, i.e., linear system; region (1) $c_A^F = c_B^F = 2$ mg/ml; region (2) $c_A^F = c_B^F = 5$ mg/ml; region (3) $c_A^F = c_B^F = 10$ mg/ml; region (4) $c_A^F = c_B^F = 15$ mg/ml.

(5), i.e., $m_{4,cr}$, is a function of c_T^F. Both behaviors are illustrated in Fig. 3. When the constraint on m_4 is not fulfilled then some amount of the weak component B is carried by the recycled mobile phase to pollute the extract product. It is worth noting that $m_{4,cr} \leq H_B$ for every value of the feed concentration, c_T^F, with the equality condition holding only in the case where the feed concentration is zero.

Now, let us analyze the effect of feed concentration on the complete separation region in the (m_2, m_3) plane. This is illustrated in Fig. 4 where the same system, i.e., same values of the adsorption equilibrium parameters, is considered but different values of the overall feed concentration, c_T^F, are adopted. Four complete separation regions using Eqs. (6)–(14) are shown, going from region L, which corresponds to the limiting situation of a feed mixture constituted of A and B infinitely diluted in the solvent, to regions 1 to 4, corresponding to larger and larger values of the feed concentration, c_T^F. It is worth noting that while increasing c_T^F the basis of the triangle-shaped region, i.e., the segment ab, remains the same, the position of the vertex w shifts downwards to the left and the complete separation region
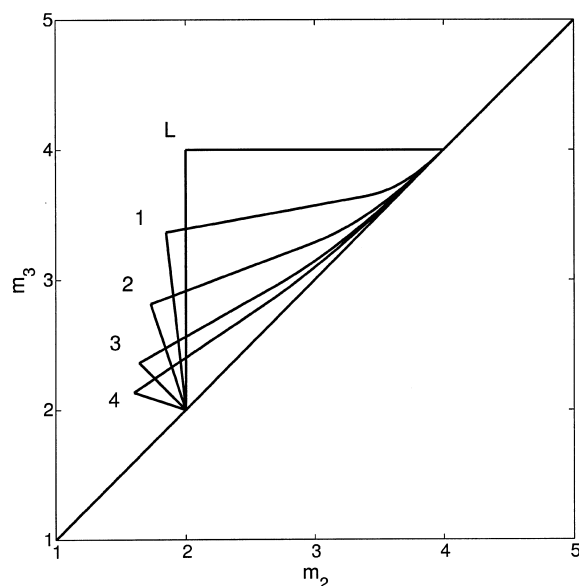
becomes sharper and sharper, i.e., less and less robust. This implies that when increasing the feed concentration the flow rate ratios in sections 2 and 3, as well as the difference $(m_3 - m_2)$ decrease, as clearly illustrated in Fig. 3. Through material balances it can be shown that maximum productivity is an increasing function of feed concentration and approaches an asymptotic value. Therefore, since productivity improves and robustness becomes poorer as feed concentration increases, then the best value of feed concentration must be chosen as a compromise between these two opposite needs [17,19].

2.3. Linear isotherm

When the feed mixture is infinitely diluted in the components to be separated the competitive Langmuir isotherm approaches the non-competitive linear isotherm (16) and the constraints on the m_j parameters of the SMB unit reduce to the following set of decoupled inequalities:

$$H_A < m_1 < \infty \tag{17}$$

$$H_B < m_2 < H_A \tag{18}$$

$$H_B < m_3 < H_A \tag{19}$$

$$\frac{-\varepsilon_p}{1-\varepsilon_p} < m_4 < H_B \tag{20}$$

These are the classical constraints for SMB separation under linear conditions [1,20]. It is worth noting that in the linear case the complete separation region is the square triangle, corresponding to region L in Fig. 4.

2.4. Choice of process operating conditions

Let us assume that a specific feed composition is given. Therefore the constraints on m_1 and m_4 as well as the complete separation region in the (m_2, m_3) plane can be determined, since these depend only on the parameters of the adsorption equilibrium isotherm and the feed composition itself. Based on these values an operating point, i.e., a set of four values of $m_j = 1, \ldots, 4$, fulfilling the complete separation requirements can be selected. The advantage of this approach is that the same constraints on the flow rate ratios, m_j, can be enforced whatever the size and productivity of the SMB unit: in fact the flow rate ratio is a dimensionless group bringing together information about volume of the columns, V, flow rates, Q_j, and switch time, t^*.

Once the four flow rate ratios are selected, two additional constraints are required in order to determine the values of the six design and process parameters involved, i.e., V, t^* and Q_j, $j = 1, \ldots, 4$. In general, the volume of the columns is given, if the plant is already available, or it is selected based on productivity requirements. A second process parameter, either t^* or equivalently Q_1, i.e., the largest flow rate in the unit, is selected by taking into account the upper boundary for pressure drop in the unit and the lower boundary for the efficiency of the columns [11,14,20]. Based on this, all the other process parameters can be calculated from the selected values of the flow rate ratios. In fact, if the volume of the columns and the switch time are known, then the flow rates in the sections of the unit are calcu-

lated by applying the definition of m_j (1), i.e., through the equation:

$$Q_j = \frac{V[m_j(1 - \varepsilon^*) + \varepsilon^*]}{t^*}. \tag{21}$$

3. Design of SMB operating conditions

3.1. Linear separations

The design of operating conditions of SMB units for the separation of mixtures characterised by linear adsorption equilibria is based on the constraints (17) to (20) above. In order to guarantee robustness of the separation the operating values of the flow rate ratios are calculated in the literature using proper safety factors, β_j, with $\beta_j > 1$, as follows [20,21]:

$$m_1 = \beta_1 H_A \tag{22}$$

$$m_2 = \beta_2 H_B \tag{23}$$

$$m_3 = H_A / \beta_3 \tag{24}$$

$$m_4 = H_B / \beta_4. \tag{25}$$

Typically in the literature the same safety factor is used for all sections, i.e., $\beta_j = \beta$, with $j = 1, \ldots, 4$. This limits the choice of operating points on a one dimensional curve in the plane (m_2, m_3) defined by values of β between 1 and $\sqrt{H_A/H_B}$. In fact, from Eqs. (23) and (24) one obtains:

$$m_2 m_3 = H_A H_B, \tag{26}$$

which corresponds to the portion of hyperbola going through the optimal point of the linear complete separation triangle and point ($\sqrt{H_A H_B}$, $\sqrt{H_A H_B}$), as illustrated in Fig. 5. Since the complete separation region is actually a bi-dimensional triangle the choice of a one-dimensional subset of it appears rather arbitrary.

This constraint is removed when different values of the safety factors in the different sections are used, as suggested and discussed recently by Zhong and Guiochon [22]. However, the procedure based on such safety factors remains ambiguous and unable to lead to the best operating conditions. These
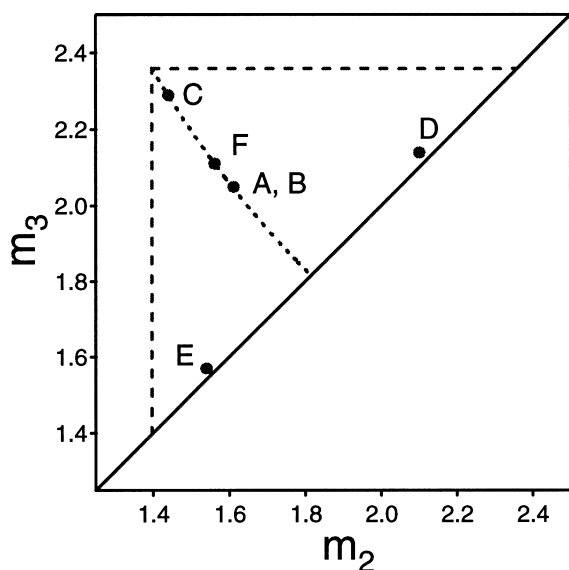
Fig. 5. Separation of 3-phenyl-1-propanol and 2-phenyl ethanol [21,22]; region of complete separation under linear conditions and experimental operating points (see Table 1). The hyperbola given by Eq. (26) is drawn as a dotted line.

limitations are already present in the case of linear equilibria and become even more severe for non-linear equilibria. In the following we illustrate how these limitations are overcome using the approach based on the 'Triangle Theory' by performing the design of a given separation in parallel using both strategies. In particular for the linear case we consider the same example used in [22], which deals with the separation of 3-phenyl-1-propanol (component A) and 2-phenyl ethanol (component B) on 10-μm Zorbax spherical C-18 bonded silica, with a 60:40 methanol/water (v/v) solution as mobile phase, in an 8-column (1.0 cm×9.8 cm) 4-section SMB unit (2-2-2-2 configuration). The adsorption

isotherms are linear in the range of concentration considered, with $H_A = 2.359$ and $H_B = 1.397$. In this and a companion paper [21] six different operating conditions have been considered as reported in detail in Table 1. Runs A to E are taken from [22], and they are labelled according to the notation of Table 3b in that paper, whereas run F corresponds to the results illustrated in Fig. 2(a) and 2(b) of [21]. It is worth noting that the feed composition is different in the different runs, but contrary to the case of nonlinear systems, changes of feed composition have no effect in the case of linear systems.

Using the data in Table 1, the values of the flow rate ratios can be calculated (the values of the overall void fraction ε^* are also given in the Table, since different values were used in different runs [21,22]). In all runs the constraints on m_1 and m_4, i.e., Eqs. (17) and (20), are fulfilled, as well as the constraints on m_2 and m_3. This can be verified by noting that all operating points in the (m_2, m_3) plane fall within the complete separation region calculated with the relevant values of the Henry constants and drawn in Fig. 5. It can also be noted that points A, B, C and F lie on the line defined by Eq. (26), and in fact in these runs $\beta_2 = \beta_3$ were used. The purity values which can be derived from the Figures reported by Zhong and Guiochon are all very close to 100%, thus in agreement with the fact that all operating parameters fulfill the complete separation constraints. Looking at Fig. 5 it is clear that when different values of the safety factors are used in different sections, there is no point in introducing the safety factors themselves. A simpler and more effective approach is to use the original inequalities (17) to (20) rather than Eqs. (22)–(25) and to select the location of the operating points inside the complete separation triangle in the (m_2, m_3) plane.

Table 1
Separation of 3-phenyl-1-propanol and 2-phenyl ethanol [21,22][a]

Run	c_A^F (g/l)	c_B^F (g/l)	t^* (min)	Q_1 (ml/min)	Q_2 (ml/min)	Q_3 (ml/min)	Q_4 (ml/min)	ε^*	E_A	E_B
A	0.091	0.115	9.33	1.436	1.04	1.201	0.902	0.572	0.405	0.535
B	0.132	0.150	9.38	1.327	1.035	1.195	0.948	0.580	0.548	0.648
C	0.127	0.130	9.38	1.327	0.971	1.286	0.948	0.580	0.885	0.932
D	–	–	9.38	1.336	1.211	1.234	0.944	0.572	0.184	0.079
E	–	–	9.38	1.336	1.014	1.031	0.950	0.572	0.052	0.210
F	0.564	0.112	6.31	2.104	1.518	1.818	1.351	0.569	0.512	0.642

[a] Operating conditions and calculated product enrichment of the experimental runs (A, B, C, F) and of the numerical simulations (D, E).

In the last two columns of Table 1 the values of the enrichment in the product streams is reported. These are defined as the ratio of the average outlet concentration over the feed concentration of the desired component. It is worth noting that this parameter is closely related to the concentration profile hence to the maximum concentration observed in the SMB unit; therefore discussing the effect of operating conditions on enrichment is equivalent to analysing their effect on concentration profiles. In the case of complete binary separation the enrichments of A and B are calculated through overall material balances and can be conveniently cast in terms of flow rates or flow rate ratios as follows:

$$E_A = \frac{c_A^E}{c_A^F} = \frac{Q_3 - Q_2}{Q_1 - Q_2} = \frac{m_3 - m_2}{m_1 - m_2}, \tag{27}$$

$$E_B = \frac{c_B^R}{c_B^F} = \frac{Q_3 - Q_2}{Q_3 - Q_4} = \frac{m_3 - m_2}{m_3 - m_4}, \tag{28}$$

The values calculated using these equations in Table 1 are consistent with the concentration profiles reported in [21,22]. The effect of changing operating conditions on these concentration profiles, particularly on maximum concentration and average enrichment, can be easily explained based on the equations above. First, since maximum enrichment can be achieved in the optimal point of the complete separation region, it is readily seen that the best experimental enrichment values are observed in run C, which is the closest to the optimal point. Moreover. when $\beta_j = \beta$, with $j = 1, \ldots, 4$, from Eqs. (22)–(25) and Eqs. (27) and (28) one obtains:

$$E_A = \frac{E_B}{\beta^2} = \frac{1}{\beta^2} \frac{H_A - \beta^2 H_B}{H_A - H_B}, \tag{29}$$

which indicates that the selection of the same value of the safety factor in all sections yields an unbalance in the enrichment values for the two components; this is larger the larger the distance of the operating point from the vertex of the complete separation triangle. This is also observed in the data of Table 1, where the values of E_A and E_B differ of about 5%, 25% and 32% in runs C, F and A, respectively (note that run B differs from run A,

because in run B $\beta_1 = \beta_4 = 1.03$, $\beta_2 = \beta_3 = 1.15$ and Eq. (29) cannot be applied).

Finally, it appears that rather small values of E_A and E_B are observed in runs D and E, whose corresponding operating points in the (m_2, m_3) plane are very close to the diagonal. Zhong and Guiochon explain this result with the small value of the feed flow rate with respect to the other runs. This is only partially correct, as it can be seen again by referring to the definitions (27) and (28). To this aim, let us assume for the sake of simplicity but without loss of generality that m_1 and m_4 have a constant value which is above and below the corresponding critical value, respectively, of the same rather small quantity, i.e., $m_1 = H_A + h$ and $m_4 = H_B - h$. It can readily be seen that along the straight line:

$$m_3 = H_A + H_B - m_2, \tag{30}$$

which goes through the vertex of the complete separation triangle and is perpendicular to the diagonal, the enrichment in the two product streams is exactly the same. In the upper part of the triangle with respect to this line the enrichment is larger in the extract than in the raffinate and vice versa in the lower part. It is worth noting that for a fixed value of t^* in a given SMB unit, the points on the line defined by Eq. (30) represent operating conditions with a feed flow rate value going from zero to the maximum one corresponding to the vertex of the triangle. Therefore, for any value of the feed flow rate there is an operating point in the complete separation region which allows to reach the same enrichment in both outlet streams. On the contrary, the distance of the operating point from the diagonal has an effect on how different E_A and E_B can be one from the other for operating points far from line (30). As an example this can be seen by considering under the same assumptions which led to Eq. (30) the operating points where $m_3 = H_A$, i.e., along the upper boundary of the complete separation triangle. From Eqs. (27) and (28) the ratio between the two enrichment values is given by:

$$\frac{E_A}{E_B} = \frac{H_A - m_4}{m_1 - m_2} = \frac{H_A - H_B + h}{H_A + h - m_2}; \tag{31}$$

this ratio increases from 1 to $1 + (H_A - H_B)/h$ as m_2 increases from H_B to H_A, thus showing that a larger

imbalance between the two values of enrichment can be obtained for operating points close to the diagonal. The same behavior, though for values of E_B larger than E_A, is obtained along the left hand boundary of the complete separation triangle where $m_2 = H_B$. In this case:

$$\frac{E_B}{E_A} = \frac{m_1 - H_B}{m_3 - m_4} = \frac{H_A - H_B + h}{m_3 - H_B + h}, \tag{32}$$

which increases from 1 to $1 + (H_A - H_B)/h$ as m_3 decreases from H_A to H_B.

The above analysis indicates that the use of the 'Triangle Theory', even in the simple case of linear equilibria provides very useful tools to rationalise and understand the results obtained through experiments or simulations and to give clear indications on how to properly design a given separation.

3.2. Nonlinear separations

The design of operating conditions of SMB units for the separation of mixtures characterised by nonlinear adsorption equilibria of the Langmuir type can be done following the approach summarised in Section 2. In a recent paper Zhong and Guiochon investigated a different strategy, based on adapting the linear design criterion described in the previous section to the nonlinear case [10]. The case study considered refers to the separation of a binary mixture described by the competitive Langmuir isotherm (2), with $H_A = 4$, $H_B = 2$, $K_A = K_B = 0.1$ ml/mg. Five different feed compositions, namely infinite dilution, i.e., $c_A^F = c_B^F = 0$ mg/ml, $c_A^F = c_B^F = 1$ mg/ml, $c_A^F = c_B^F = 2$ mg/ml, $c_A^F = c_B^F = 4$ mg/ml and $c_A^F = c_B^F = 8$ mg/ml are considered. Columns with an overall void fraction $\varepsilon^* = 0.333$ are used. The operating conditions in the numerical experiments are chosen following the linear criterion defined by Eqs. (22)–(25), with the same safety factor, β, for all sections. The authors analyse the effect of the different feed compositions and of different values of the safety factor, namely $\beta_A = 1.05$, $\beta_B = 1.10$, $\beta_C = 1.15$, $\beta_D = 1.20$, $\beta_E = 1.25$, $\beta_F = 1.30$.

Once the value of the safety factor is fixed, then the values of the flow rate ratios are known from Eqs. (22)–(25), and the corresponding operating points in the operating parameter space can be

located as illustrated in Fig. 6. They belong to the curve given by Eq. (26). In the same figure the complete separation triangles calculated for the different feed compositions as shown in Section 2.1 are drawn (region L corresponds to infinite dilution linear conditions, whereas the other regions are labelled with the number corresponding to the value of the feed concentration in g/l). As discussed in Section 2.4, the choice of the flow rates and the switch time requires an additional constraint. To this aim, Zhong and Guiochon use the same value of the feed flow rate, Q_F, in all simulations. For every selected value of the safety factor, i.e.. from β_A to β_F, material balances at the nodes of the unit together with Eq. (1) and Eqs. (22)–(25) yield the following relationships:

$$\frac{t^* Q_F}{V(1 - \varepsilon^*)} = H_A/\beta - \beta H_B \tag{33}$$
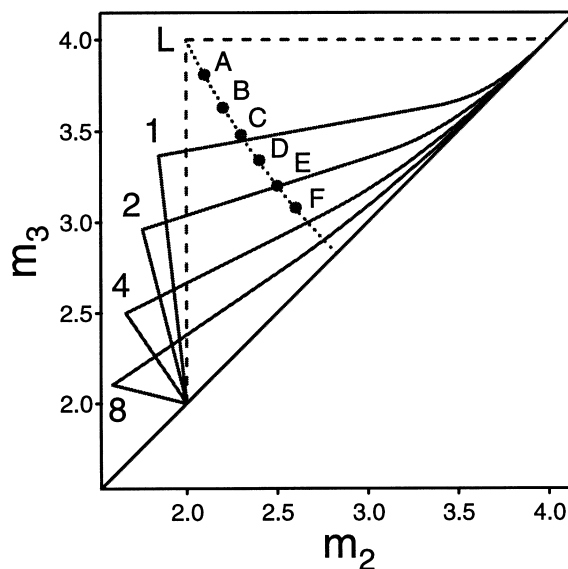

Fig. 6. Separation of a model system characterized by the Langmuir adsorption isotherm (parameters as in Fig. 3) [10]. Regions of complete separation corresponding to different feed composition: region L, $c_A^F = c_B^F = 0$ mg/ml; region 1, $c_A^F = c_B^F = 1$ mg/ml; region 2, $c_A^F = c_B^F = 2$ mg/ml; region 4, $c_A^F = c_B^F = 4$ mg/ml; region 8, $c_A^F = c_B^F = 8$ mg/ml. Operating points of the numerical experiments, corresponding to operating conditions reported in Table 2. The hyperbola given by Eq. (26) is drawn as a dotted line.

$$\frac{Q_j}{Q_F} = \frac{m_j + \varepsilon^*/(1 - \varepsilon^*)}{H_A/\beta - \beta H_B}. \tag{34}$$

The operating conditions of the thirty numerical experiments performed by Zhong and Guiochon and calculated using the last two equations are reported in Table 2; each letter refers to a value of the safety factor, β, and corresponds to an operating point in the operating parameter space. It is worth noting that different values of β correspond to very different values of the flow rates in the different sections of the unit (note that according to Eq. (34) flow rates in sections 2 and 3 in run F are about four and three times larger, respectively, than in run A). Accordingly, these operations cannot be really compared in

practice since pressure drop and column efficiency are vastly different.

In the last two columns of Table 2 the calculated separation performances in terms of purity of the outlet streams are also reported. No numerical values are given in [10], therefore a boolean notation based on the concentration profiles reported in [10] has been adopted: 1 indicates 100% purity, whereas 0 indicates that 100% purity has not been achieved.

Let us now show how these results can be rationalised in the light of the nonlinear criteria presented in Section 2.1, which can also be used to derive optimal operating conditions for the unit. Before considering the relative position of the operating points with respect to the complete separation

Table 2
Separation of a model system characterized by the Langmuir adsorption isotherm [10][a]

Run	$c_A^F = c_B^F$ (g/l)	$(t^*Q_F)/(V(1-\varepsilon^*))$	Q_1/Q_F	Q_2/Q_F	Q_3/Q_F	Q_4/Q_F	$m_4 - m_{4,cr}$	P_E	P_R
A ($\beta = 1.05$)	0	1.71	3.63	2.40	3.40	2.28	−0.1	1	1
	1						0.06	0	0
	2						0.18	0	0
	4						0.46	0	0
	8						0.60	0	0
B ($\beta = 1.10$)	0	1.43	4.46	2.92	3.92	2.66	−0.19	1	1
	1						−0.04	1	0
	2						0.08	0	0
	4						0.25	0	0
	8						0.47	0	0
C ($\beta = 1.15$)	0	1.18	5.60	3.65	4.65	3.17	−0.26	1	1
	1						−0.12	1	0
	2						−0.02	1	0
	4						0.14	0	0
	8						0.36	0	0
D ($\beta = 1.20$)	0	0.94	7.29	4.71	5.71	3.92	−0.33	1	1
	1						−0.21	1	1
	2						−0.11	1	0
	4						0.03	0	0
	8						0.24	0	0
E ($\beta = 1.25$)	0	0.70	10	6.43	7.43	5.14	−0.40	1	1
	1						−0.30	1	1
	2						−0.22	1	1
	4						−0.08	1	0
	8						0.10	0	0
F ($\beta = 1.30$)	0	0.48	15.1	9.64	10.64	7.42	−0.46	1	1
	1						−0.38	1	1
	2						−0.31	1	1
	4						−0.21	1	0
	8						−0.05	1	0

[a] Operating conditions of the numerical experiments; difference between the flow rate ratio m_4 and the corresponding critical value given by Eq. (5); purity of the outlet streams calculated in the numerical experiments [10]. The purity is indicated using a boolean notation: 1 corresponds to 100% purity, while 0 corresponds to purity smaller than 100%.

regions in the (m_2, m_3) plane, it is necessary to check the fulfilment of the constraints on the flow rate ratios in the regenerating sections 1 and 4. Since β is always larger than 1, comparing Eq. (22) and the constraint on m_1 Eq. (3) shows that the latter is fulfilled in all experiments. Hence the stationary phase is properly regenerated and no strong component A is carried by the solid phase to pollute the raffinate stream. However, it should be noted that according to the procedure based on safety factors [22] the value of m_1 is proportional to β, which is increased from run A to F to try to cope with the increasing nonlinearity induced by the increasing feed concentration. This implies that m_1 is unnecessarily increased in runs B to F, since the value of m_1 adopted in run A is already large enough to regenerate the stationary phase and the lower bound on m_1, does not depend on the feed concentration. On the other hand this has the negative effect of producing an excessive dilution of the product streams, particularly of the extract (see Eq. (27)).

On the contrary, according to Eq. (5) the critical value of the flow rate ratio in section 4 m_4, which guarantees complete adsorption of the weak component B and regeneration of the mobile phase before recycle to section 1, is a function of the flow rate ratios in section 2 and 3 and of feed composition. Therefore, this critical value is different for all operating conditions, whereas the operating value of m_4 chosen according to the safety factor criterion according to Eq. (25) depends only on β and therefore is the same for all simulations with the same letter label. To clarify this point the value of the difference $(m_4 - m_{4,cr})$ is reported in Table 2; when this value is negative the constraint (5) is fulfilled and the mobile phase is properly regenerated, whereas in the opposite case some amount of component B pollutes the extract. Accordingly, all runs in Table 2 where this difference is positive exhibit a non pure extract stream. This is a very simple way to explain the poor extract purity observed in run A with c_A^F from 1 to 8 mg/ml, in run B with c_A^F from 2 to 8 mg/ml, in run C with c_A^F from 4 to 8 mg/ml and in run E with $c_A^F = 8$ mg/ml. It is worth stressing that without using the 'Triangle Theory' approach, in the form of the constraints (3) and (5), it would have not been possible to explain or to predict a priori such poor performances, since

the safety factor approach does not provide any conditions for the proper operation of sections 1 and 4 under nonlinear overload conditions.

Let us now consider the position of the operating points in the (m_2, m_3) plane as illustrated in Fig. 6. First of all, it has to be observed that the line where the operating points A to F have been selected, i.e., curve (26), is completely different from the line which connects the optimal operating points of the complete separation triangles calculated at different values of the overall feed concentration, which is given by the line connecting the vertices of such triangles. The comparison between the two loci is not straightforward; in fact the latter represents exact optimal operating conditions for the different values of feed concentration and the nonlinear adsorption isotherm under consideration. On the contrary the former is obtained by increasing the safety factor, β, aiming at empirically matching the nonlinear constraints through a one- dimensional search along curve (26). It is apparent that following the safety factor approach one cannot find the optimal operating conditions for nonlinear operations. In addition. by increasing β smaller values of m_3 and larger values of m_2 are obtained, contrary to what are actually required, as shown by the exact nonlinear criterion, which asks for smaller values of both m_2 and m_3 when c_T^F increases as given by Eq. (14) (see also Fig. 3).

On top of these rather general remarks, it is worth analysing the performance achieved in the different numerical experiments. First of all, it can be readily observed that all experiments at infinite dilution achieve complete separation, since points A to F belong to the linear complete separation triangle, i.e., region L. Let us now consider run A with feed concentration from 1 to 8 mg/ml. Point A belongs to none of the complete separation regions corresponding to these feed concentrations; actually it is always within the pure extract region (cf. Fig. 2). As a consequence, the raffinate purity is always poor as observed in [10] and reported in Table 2. However, since the constraint on m_4 is never fulfilled in these four cases, the extract stream is also polluted and both components A and B distribute in the two outlet streams. It is worth pointing out that this occurs for two different reasons: component A pollutes the raffinate because the operating point is in the pure

extract region in the (m_2, m_3) plane and component B pollutes the extract because the constraint on m_4 Eq. (5) is not fulfilled. It is evident that such an ability to identify clearly the causes of poor separation performance is of tremendous help in applications; based on this the practitioner derives suggestions on how to change the flow rates in the unit to achieve the desired separation performance. The approach based on safety factors does not provide any quantitative indication on how to change the operating conditions and the practitioner is left with qualitative information about the position and propagation rates of concentration fronts such as those discussed by Zhong and Guiochon.

Similar arguments as for run A can be applied for runs B and C with feed concentration from 1 to 8 mg/ml. In this case three runs fulfill the constraint on m_4 and accordingly they produce pure extract. These are run B at 1 mg/ml and run C at 1 and 2 mg/ml. Let us consider the operating points D, E and F and their position in the (m_2, m_3) plane in Fig. 6; all of them belong to the complete separation region corresponding to $c_A^F = c_B^F = 1$ mg/ml and the last two also to that corresponding to $c_A^F = c_B^F = 2$ mg/ml. Accordingly, the corresponding calculations performed at these feed concentrations lead to complete separation, because under these conditions also the constraint on m_4 is fulfilled (cf. Table 2). In contrast, these three operating points belong to the pure extract region for feed concentration equal to 4 and 8 mg/ml (point D also when $c_A^F = c_B^F = 2$ mg/ml). Accordingly, the raffinate stream is not pure in all the corresponding calculations.

From the above analysis it appears that the method based on safety factors proposed by Zhong and Guiochon cannot be applied to determine optimal operating conditions of SMB units for the separation of mixtures characterised by nonlinear competitive adsorption isotherms. For example, in the case of $c_A^F = c_B^F = 2$ mg/ml it is possible to take $\beta = 1.25$, i.e., point E, to achieve complete separation; in the case of the largest feed concentration value, i.e., $c_A^F = c_B^F = 8$ mg/ml it is possible to calculate that the first point along the line $m_2 m_3 = H_A H_B$ in Fig. 6 which falls within the complete separation region 8 corresponds to $\beta = 1.38$, i.e., rather close to the maximum β value of 1.41. However, it is evident from Fig. 6 that in both cases the operating point chosen with this approach is rather far from the optimal operating

point selected through the nonlinear 'Triangle Theory' approach.

4. Concluding remarks

Simulated Moving Bed technology is achieving high separation performance in a larger and larger number of fine chemical and enantiomer separation thanks to two main features: the highly efficient countercurrent contact between the stationary and the mobile phase and the overload conditions under which SMBs are operated, leading to nonlinear competitive adsorption behavior. The fast and optimal design of new applications requires that the nonlinear character of the separation is properly accounted for. The so called 'Triangle Theory', which was developed from Equilibrium Theory, i.e., neglecting mass transfer resistance and axial dispersion, achieves this objective. In fact, it provides exact criteria to locate the region in the operating parameter space, which allows to achieve the desired separation performance, and to determine the optimal operating point, where productivity per unit mass of stationary phase and eluent consumption are optimised. In the case of Langmuir isotherms these criteria require the use of a few algebraic relationships. The effect of increasing system nonlinearity by increasing feed concentration can be understood and predicted for optimisation purposes.

Based on this, 'Triangle Theory' allows an explanation of experimental results, troubleshooting of pilot SMB units, evaluation of alternative solutions in terms of stationary and mobile phases and performance of 'educated' analysis of SMB performance under nonideal conditions using detailed models. In particular the approach has already been applied to the analysis of experimental results obtained in different laboratories for the separation of the alkylaromatic C_8 fraction [12,13,23], linear and nonlinear paraffins [15,24], the Sandoz epoxide [17], a chiral intermediate [17], the enantiomers of guaifenesin [25], the enflurane enantiomers [5], the Tröger's base enantiomers [4] and the enantiomers of binaphtol [11].

In this paper the design of linear and nonlinear SMBs is discussed. It has been proved that in the linear case the 'Triangle Theory' approach provides better insight than a strategy based on the use of

safety factors, even though both methods are able to locate the optimal operating conditions. For the nonlinear case, an extension of this safety factor strategy has been recently proposed and analysed [10]. However, the analysis developed in this work demonstrates that the 'Triangle Theory' approach outperforms this last strategy; in fact the safety factor method is not able to locate the optimal operating conditions and to explain the separation performance achieved in a rather large number of numerical experiments [10]. In contrast, 'Triangle Theory' determines exactly the optimal operating conditions as a function of adsorption isotherm parameters and feed composition and explains the whole set of numerical experiments on a quantitative basis. The possibility of applying such powerful analysis and useful design tool is expected to promote the application of SMB technology to a larger and larger number of new applications.

5. Notation

c	Fluid phase weight concentration
E	Enrichment, defined by Eqs. (27) and (28)
H	Henry constant
K	Adsorption equilibrium constant
m_j	Mass flow ratio in section j, defined by Eq. (1)
n	Adsorbed phase weight concentration
P_E	Desorbent free Extract purity
P_R	Desorbent free Raffinate purity
Q	Volumetric flow rate
t^*	Switch time in a SMB unit
V	Volume of the column

Greek letters

β	Safety factor, $\beta \geq 1$
ε	Void fraction of the bed
ε_p	Intraparticle void fraction
ε^*	Overall void fraction, $\varepsilon^* = \varepsilon + \varepsilon_p(1-\varepsilon)$
ω	Equilibrium Theory parameter defined by Eq. (15)

Subscripts and superscripts

A	More retained component in the feed
B	Less retained component in the feed
E	Extract
F	Feed
j	Section index
R	Raffinate
S	Eluent
T	Overall quantity

References

[1] D.M. Ruthven, C.B. Ching, Chem. Eng. Sci. 44 (1989) 1011.
[2] J.N. Kinkel, M. Schulte, R.M. Nicoud, F. Charton, in Proceedings of the Chiral Europe '95 Symposium, Spring Innovations Limited, Stockport, UK, (1995) p. 121.
[3] M.J. Gattuso, B. McCulloch, J.W. Priegnitz, Chem. Tech. Eur. 3(3) (1996) 27.
[4] M.P. Pedeferri, G. Zenoni, M. Mazzotti, M. Morbidelli, Chem. Eng. Sci., submitted for publication (1998).
[5] M. Juza, O. Di Giovanni, G. Biressi, V. Schurig, M. Mazzotti, M. Morbidelli, J. Chromatogr. A 813 (1998) 333.
[6] C.B. Ching, D.M. Ruthven, Chem. Eng. Sci. 40 (1985) 1411.
[7] G. Storti, M. Masi, R. Paludetto, M. Morbidelli, S. Carr, Comput. Chem. Eng. 12 (1988) 475.
[8] G. Storti, M. Masi, S. Carrà, M. Morbidelli, Chem. Eng. Sci. 44 (1989) 1329.
[9] L.S. Pais, J.M. Loureiro, A.E. Rodrigues, J. Chromatogr. A 769 (1997) 25.
[10] G. Zhong, G. Guiochon, Chem. Eng. Sci. 52 (1997) 4403.
[11] C. Migliorini, A. Gentilini, M. Mazzotti, M. Morbidelli, Ind. Eng. Chem. Res., submitted for publication (1998).
[12] G. Storti, M. Mazzotti, M. Morbidelli, S. Carrà, American Institute of Chemist Engineers Journal (AIChE J.) 39 (1993) 471.
[13] M. Mazzotti, G. Storti, M. Morbidelli, AIChE J. 40 (1994) 1825.
[14] G. Storti, R. Baciocchi, M. Mazzotti, M. Morbidelli, Ind. Eng. Chem. Res. 34 (1995) 288.
[15] M. Mazzotti, G. Storti, M. Morbidelli, AIChE J. 42 (1996) 2784.
[16] M. Mazzotti, G. Storti, M. Morbidelli, AIChE J. 43 (1997) 64.
[17] M. Mazzotti, G. Storti, M. Morbidelli, J. Chromatogr. A 769 (1997) 3.
[18] A.S.T. Chiang, AIChE J. 44 (1998) 332.
[19] A. Gentilini, C. Migliorini, M. Mazzotti, M. Morbidelli, J. Chromatogr. A 805 (1998) 37.
[20] F. Charton, R.-M. Nicoud, J. Chromatogr. A 702 (1995) 97.
[21] T. Yun, G. Zhong, G. Guiochon, AIChE J. 43 (1997) 935.
[22] G. Zhong, G. Guiochon, AIChE J. 43 (1997) 2970.
[23] G. Storti, M. Mazzotti, L.T. Furlan, M. Morbidelli, in: M. Suzuki, (Ed.), Fundamentals of Adsorption, Kodansha, Tokyo, 1993, p. 607.
[24] M. Mazzotti, R. Baciocchi, G. Storti, M. Morbidelli, Ind. Eng. Chem. Res. 35 (1996) 2313.
[25] E. Francotte, P. Richert, M. Mazzotti, M. Morbidelli, J. Chromatogr. A 796 (1998) 239.